Microwave Review
July 2026, Vol. 32, No. 1, pp. 3-7
DOI: 10.18485/mtts_mr.2026.32.1.1

An Ultra-Low-Cost Wideband Broadside Antenna Using Metallic Additive Manufacturing for Ka-Band Applications

Vikas K, Karthikeya G. S and Varun C. V

Abstract – **In this paper, a wideband broadside antenna designed to operate in the mmWave 5G bands is proposed. The antenna is realized with an aperture-coupled topology. The feed plane is designed on a commercially viable low-cost substrate. The feed plane is integrated with a metallic additively manufactured dipole arm. The overall fabricated assembly is inexpensive and simple to realize. The proposed wideband antenna offers an impedance bandwidth of 45% with an effective radiating volume of $0.109\lambda^3$. The proposed antenna offers unidirectional patterns across the operating spectrum with a forward gain of 5dBi and beyond. The cross-polarization level is below 18dB across the band. The isolation is relatively higher in the H-plane. Detailed characteristic results are presented in this paper.**

Keywords – **Aperture coupled, mmWave 5G, Low-cost, Additive manufacturing**

I. INTRODUCTION

With the onset of commercial 5G networks, there is a huge demand in the wireless industry to design, develop and deploy high frequency networks. This growth was fuelled by the demonstrations of mmWave carrier frequencies for commercial applications [1]. One of the primary design hurdles to realize these radios is the relatively high free space path loss. For instance, the free space path loss (FSPL) for a 200 m link at 2.4 GHz is 86 dB. On the other hand, the FSPL is 107 dB at 28 GHz. The solution to mitigate this problem is to increase transmitter power, which would lead to higher power loss. The other feasible option is to design high gain antennas, to be integrated with the transceivers, as demonstrated in [2].

As the operating frequency is high, the physical footprint of the antenna would be relatively low, which in turn would meet the dimensional constraints laid down by the transceivers. One of the common problems with high gain antenna design is the relatively low impedance bandwidth. The impedance bandwidth could be enhanced by realizing an end-fire radiating element, such as a printed dipole characterized on an expensive low-loss substrate [3]. A traveling wave antenna also could be used to simultaneously enhance the on-axis gain and the impedance bandwidth, as illustrated in [4].

Article history: Received January 16, 2026; Accepted March 27, 2026

Vikas K, Karthikeya G. S and Varun C. V are with the Department of Electronics and Communication Engineering, B.M.S College of Engineering, P.O. Box No.: 1908 Bull Temple Road, Bangalore - 560 019, E-mail: karthikeya.ece@bmsce.ac.in

The electrical footprint of this design approach would be high. The gain of a single element planar end-fire radiator could be enhanced by integration of phase-correcting structures, such as metamaterial unit cells in the effective radiating space of the antenna. Design examples of this approach have been reported in the past [5]-[6]. The primary limitation with such designs is that the phase-correcting structures are a function of the operating wavelength, which in-turn leads to narrow impedance bandwidth. Another approach for end-fire antenna gain enhancement is to design an electrically large dielectric lens [7].

The impedance bandwidth is dictated by the geometry of the expensive lens. Variants of the sub-wavelength unit cell integration is illustrated in [8], [9]. The impedance and gain bandwidths are restricted. The other alternative to realize wide impedance bandwidth in the mmWave frequencies is to design a slotted radiator, as illustrated in [10], [11]. The fabrication and assembly of these structures are challenging to realize. Even though wideband, broadside radiators have been demonstrated in the past, they are either expensive or challenging to fabricate [12-15]. A multi-layered high gain antenna array is presented in [16]. The feed layer requires precision engineering to realize the design. A parasitically coupled design is presented in [17], the fabrication process requires multiple steps. Here, the parasitically coupled geometry enhances the operational bandwidth to 30%.The boresight gain is around 12dBi. A multi-layered stacked dual-polarized antenna array is demonstrated in [18]. Here, the topology of the ME dipole is realized using vias and slots within the stacked architecture. An array topology of the dual-polarized design is also explored. The design achieves a boresight gain of 22dBi for a 4x8 array. A high radiation efficiency Ka-band antenna array is presented in [19], which requires metallic additively manufacturing technology with capability to print thin walls. A wideband antenna operating in the D-band is proposed in [20]. In this paper, an ultra-low-cost wideband broadside antenna operating in the Ka-band is presented.

II. PROPOSED ANTENNA DESIGN

The schematics of the proposed ultra-low-cost wideband broadside antenna using metallic additive manufacturing is illustrated in Fig. 1. The antenna is composed of two parts, the first part is the feed, which is realized using conventional feeding technique to interface the standard 50 Ω port. The second part is the primary radiating element, which is realized using a patterned geometry of metallic structure. The feed is

designed on an ultra-low-cost substrate, FR4 (Flame Retardant) which has a dielectric constant of 4.4 and a corresponding loss tangent of 0.04. The thickness of the substrate is 0.5mm, translating to 0.046 λ, λ computed at 28 GHz. Even though the substrate is lossy at higher frequencies, the effect of the dielectric loss tangent is mitigated with the use of electrically thin substrate. The choice of thickness of this feed plane is a compromise between the dielectric loss and the mechanical strength to fasten the metallic structures.

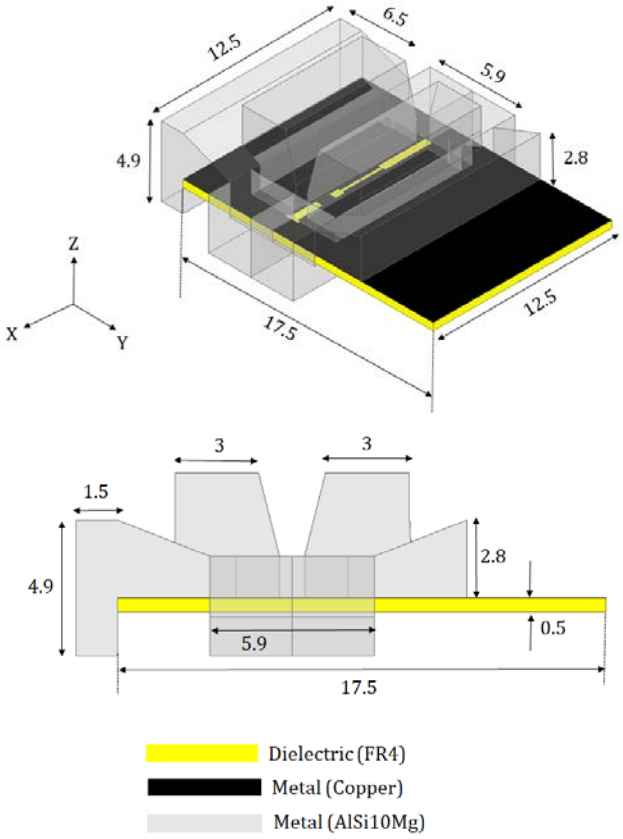

Fig. 1. Proposed wideband broadside antenna (All dimensions are in mm)

The geometry of the feed plane is illustrated in Fig. 2. Here, a 50 Ω line is connected to an electrically small square patch, as observed in the figure. The feed is terminated by a series-loaded square patch, which is connected through a small transition, which is non-radiative in nature. The overall dimensions of the substrate is chosen to accommodate the industry standard connector and to accommodate the metallic structure on the other side of the substrate. The slots in the ground planes have a width of 0.5 mm, or 0.046 λ at 28 GHz. These asymmetric slots act as a coupler of the incident signal to the metallic structures. The geometry of the slots is optimized for wide-impedance matching in the band of interest and minimal backward radiation. The presence of two distinct slots aid in the impedance bandwidth enhancement. Once the energy is coupled to the slots in the ground planes, it is radiated by primary radiating dipole arms, which are also illustrated in Figure 1. The radiating dipole arms have an optimized half-wavelength width at the centre frequency of 24 GHz. A conventional straight or orthogonal bend dipole arms would lead to narrow bandwidth. The geometry is mostly slanted or tapered to enhance the impedance and gain bandwidth of the overall assembly of the proposed antenna system. The arrangement of the metallic structure is optimized to closely fit the substrate dimensions.

The protrusions observed in the side view of the schematics is purely for alignment purposes, and the same does not contribute to radiation, as these protrusions are beyond the feeding ground plane. It must also be noted that the minimum thickness of the radiating dipole arm is maintained at 1.5 mm due to the limitations of the DMLS (Direct Metal Laser Sintering) technology available to the authors.

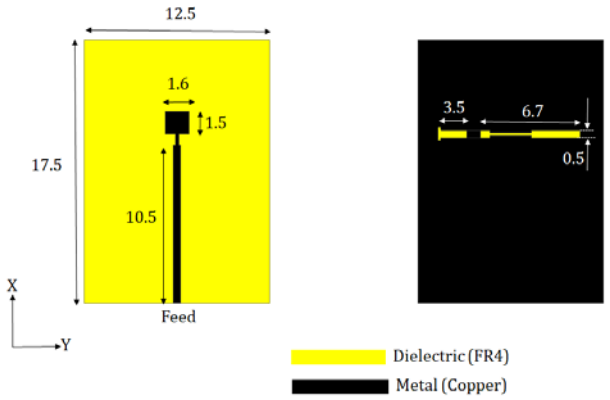

(a) (b)

Fig. 2. Schematics of the feed plane of the proposed wideband broadside antenna: (a) Top plane, (b) Ground plane

The gap between the two radiating dipole arms is maintained by the aligner designed, as part of the metallic geometry. The photograph of the fabricated and assembled prototype is shown in Fig. 3.

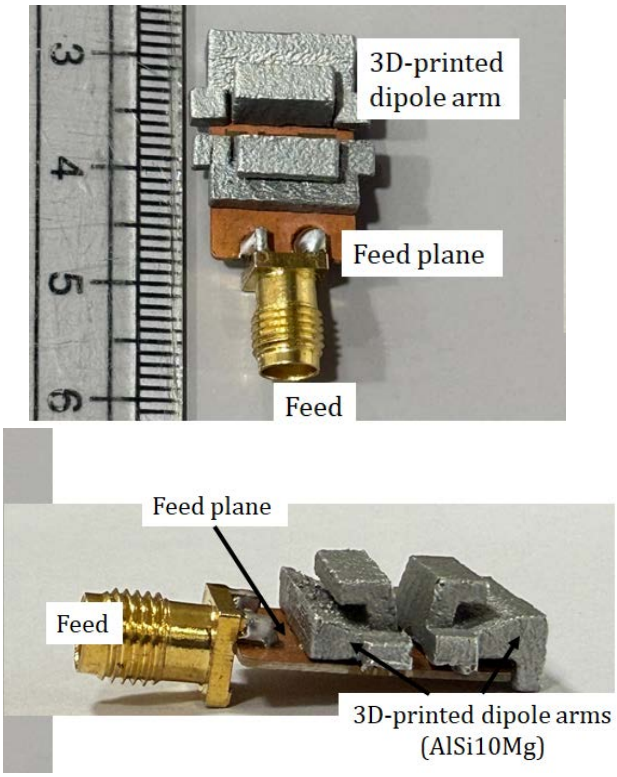

Fig. 3. Photographs of the fabricated prototype

The feed plane was fabricated using the commercial two-layer photolithography technique. As the minimum slot width is greater than 0.1 mm, the standard technique was used for fabrication. The two of the modified wideband dipole arms were independently fabricated using the DMLS technology. The metal 3D-printer EOS® M 290, was used to fabricate the geometries using AlSi10Mg alloy. The conductivity of the afore-mentioned alloy serves the purpose of radiation in the Ka-band. The metallic 3D-printed parts are fastened to the ground plane of the feed substrate using commercial adhesive, as the layer thickness of these polymers are electrically small, the contribution of the adhesive is negligible in the current context. It must be noted that the surface resolution of the additively manufactured dipole arms is 50 microns, which has a minimal influence on the performance metrics of the proposed antenna. A standard 26.5 GHz SMA connector is carefully soldered to the feed plane. It must be noted that the connector's loss beyond this frequency point is relatively low.

III. Results and Discussions

The simulated and measured input reflection coefficients of the proposed wideband broadside antenna are shown in Fig. 4.

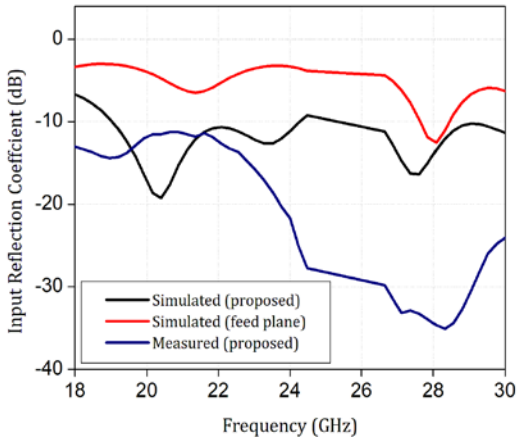

Fig. 4. Input reflection coefficient of the proposed antenna

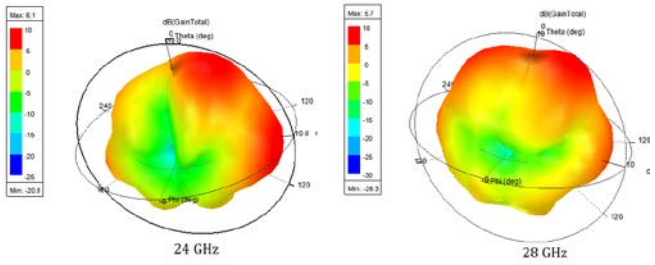

Fig. 5. 3D patterns of the proposed antenna at 24 and 28 GHz

The non-resonating nature of the feed alone with electrically small slots is also shown in the figure. The radiation from the slots alone is minimal. The -10 dB input impedance bandwidth of the proposed antenna is from 19 to 30 GHz, translating to a value of 45%, the wide bandwidth could be attributed to multiple reasons: first the design of the feeding structure, wherein the feed line couples to asymmetric slots which supports wide impedance bandwidth. The second

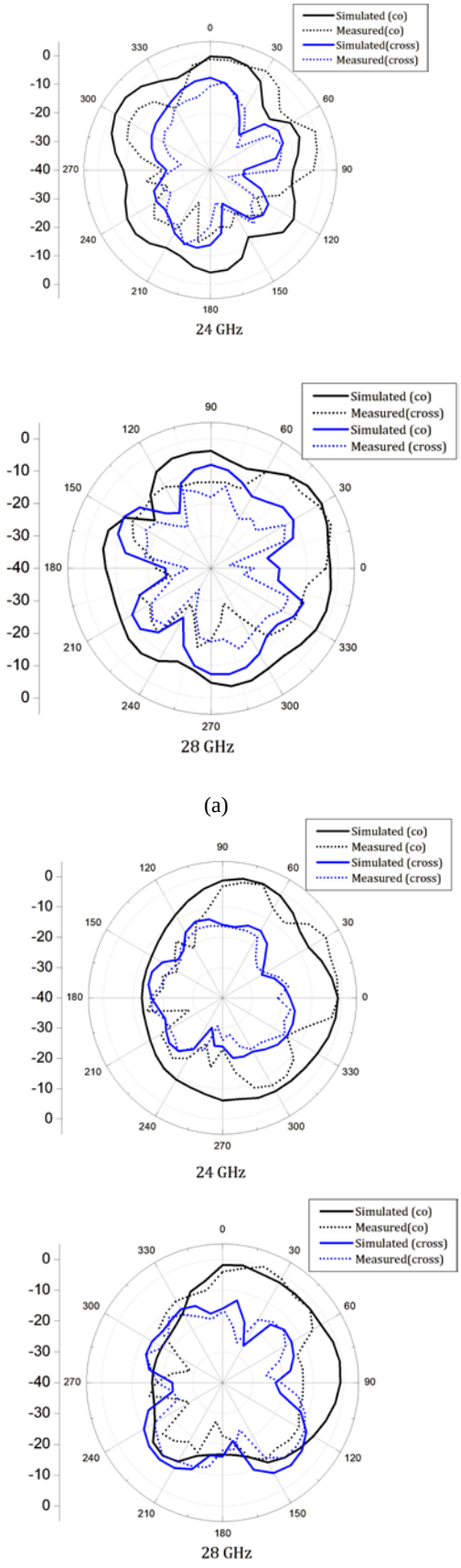

Fig. 6. Radiation patterns at 24 and 28 GHz in: (a) YZ plane, (b) XZ plane

reason is that multi-layer designs typically tend to deliver higher bandwidths compared to a conventional single layer design [12]-[13]. The third reason for wide bandwidth is the tapered design of the active radiating arms. The measurements were done with a properly calibrated Rohde & Schwarz® ZNB 40 vector network analyser. The deviations between the simulated and experimental curves are within the limits of experimental error.

The measured values seem to be better than its simulated counterpart due to the lead inductance at the feed plane. The errors within the assembly also would have created subtle deviations in the measured values. The 3D patterns of the proposed wideband antenna at key frequencies are shown in Fig. 5.

The patterns are uni-directional due to the electrically large ground plane with minimal back radiation from the non-radiating slots. The radiation patterns are almost similar to that of a narrowband resonant patch in the operating frequencies. The speckles within the radiation patterns at the edges could be attributed to the protrusions of the additively manufactured radiating arms. These protrusions aid in the assembly and influence the radiation patterns. In order to mitigate this effect, the aligner could be realized with reduced thickness with an increased cost of fabrication. The simulated and measured co and cross-polarized far-field patterns of the proposed antenna in both the principal planes are shown in Fig. 6.

The front to back ratio (FTBR) is close to 7 dB and beyond in the entire operating band. The FTBR could be improvised with an electrically large ground plane design, but would defeat the purpose of the compact broadside radiator feature. The pattern integrity is almost maintained throughput the operating band. The boresight broadside gain is depicted in Fig. 7.

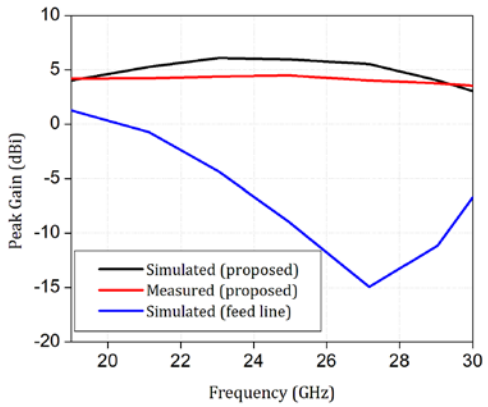

Fig. 7. Forward gain of the proposed antenna

The non-radiating nature of the feed plane is evident from the graph. The boresight gain is above 5 dBi across the band, which could be attributed to the design of the optimized additively manufactured dipole arm. Table 1 illustrates the advantages of the proposed wideband broadside antenna compared to previously reported designs. The proposed antenna delivers a high gain with relatively high -10 dB impedance bandwidth in addition to an electrically small radiating structure.

TABLE 1
COMPARISON WITH REPORTED WORKS

Ref	F	IBW	G	C	ERV	F	R	F
[5]	60	23.7	11	H	0.716	M	E	Cx
[6]	60	11.6	12	H	1.09	M	E	Cx
[7]	60	11.6	20	H	68.64	M	E	M
[8]	64	14.6	11	H	0.26	M	E	S
[9]	28	18.2	11	H	0.32	M	E	S
[10]	28	18	6.5	H	0.32	CPW	E	Cx
[11]	28	17	7	H	0.27	CPW	E	Cx
[12]	28	29	8.3	H	0.103	AC	B	S
[13]	33.5	19	20	H	NA	SIW	B	Cx
[14]	15	11.5	4	H	0.11	Coax	B	Cx
[15]	30	31	8	H	0.15	AC	B	Cx
P	**28**	**45**	**6**	**L**	**0.109**	**AC**	**B**	**S**

Ref=Reference, F=Centre frequency (GHz), IBW=10-dB impedance Bandwidth (%), G=Gain (dBi), C=Cost, H=High, L=low, F=feed, M=Microstrip, AC= Aperture-coupled, R= Radiation Type, E=End-fire, B= Broadside, ERV= Effective Radiating Volume (λ_0^3), F (Fabrication and Assembly), Cx=Complex, M= Moderate, S=Simple, P=Proposed

IV. CONCLUSION

In this paper, an ultra-low-cost wideband broadside antenna operating in the Ka-band is proposed. The antenna is an aperture coupled topology, designed using an electrically thin commercially viable substrate and additively manufactured metallic radiating arms. The antenna delivers a high impedance bandwidth of 45% with high pattern integrity across the operating band. The proposed element achieves a boresight on-axis gain of above 5dBi in the operating band. The proposed antenna might be a suitable candidate for mmWave 5G portable devices operating in different frequency bands.

REFERENCES

[1] T. S. Rappaport, S. Sun, R. Mayzus, H. Zhao, Y. Azar, K. Wang, G. N. Wong, J. K. Schulz, M. Samimi and F. Gutierrez, “Millimeter Wave Mobile Communications for 5G Cellular: It will work!”, in *IEEE Access*, vol. 1, pp. 335-349, 2013, DOI: 10.1109/ACCESS.2013.2260813

[2] W. Hong, K-H. Baek, Y. Lee, Y. Kim and S-T. Ko, “Study and Prototyping of Practically Large-Scale mmWave Antenna Systems for 5G Cellular Devices”, in *IEEE Communications Magazine*, vol. 52, no. 9, pp. 63-69, September 2014, DOI: 10.1109/MCOM.2014.6894454

[3] S. X. Ta, H. Choo and I. Park, “Broadband Printed-Dipole Antenna and Its Arrays for 5G Applications”, in *IEEE Antennas and Wireless Propagation Letters*, vol. 16, pp. 2183-2186, 2017, DOI: 10.1109/LAWP.2017.2703850

[4] B. Yang, Z. Yu, Y. Dong, J. Zhou and W. Hong, “Compact Tapered Slot Antenna Array for 5G Millimeter-Wave Massive MIMO Systems”, in *IEEE Transactions on Antennas and Propagation*, vol. 65, no. 12, pp. 6721-6727, Dec. 2017, DOI: 10.1109/TAP.2017.2700891

[5] A. Dadgarpour, B. Zarghooni, B. S. Virdee and T. A. Denidni, “Improvement of Gain and Elevation Tilt Angle Using Metamaterial Loading for Millimeter-Wave Applications”, in

IEEE Antennas and Wireless Propagation Letters, vol. 15, pp. 418-420, 2016, DOI: 10.1109/LAWP.2015.2449235

[6] A. Dadgarpour, B. Zarghooni, B. S. Virdee and T. A. Denidni, "One- and Two-Dimensional Beam-Switching Antenna for Millimeter-Wave MIMO Applications", in *IEEE Transactions on Antennas and Propagation*, vol. 64, no. 2, pp. 564-573, Feb. 2016, DOI: 10.1109/TAP.2015.2508478

[7] Z. Briqech, A. Sebak and T. A. Denidni, "Wide-Scan MSC-AFTSA Array-Fed Grooved Spherical Lens Antenna for Millimeter-Wave MIMO Applications", in *IEEE Transactions on Antennas and Propagation*, vol. 64, no. 7, pp. 2971-2980, July 2016, DOI: 10.1109/TAP.2016.2565704

[8] M. Sun, Z. N. Chen and X. Qing, "Gain Enhancement of 60-GHz Antipodal Tapered Slot Antenna Using Zero-Index Metamaterial", in *IEEE Transactions on Antennas and Propagation*, vol. 61, no. 4, pp. 1741-1746, April 2013, DOI: 10.1109/TAP.2012.2237154

[9] Z. Wani, M. P. Abegaonkar and S. K. Koul, "Millimeter-Wave Antenna with Wide-Scan Angle Radiation Characteristics for MIMO Applications", in *International Journal of RF and Microwave Computer-Aided Engineering*, 2018, DOI: 10.1002/mmce.21564

[10] G. S. Karthikeya, M. P. Abegaonkar, and S. K. Koul, "CPW Fed Conformal Folded Dipole with Pattern Diversity for 5G Mobile Terminals", in *Progress in Electromagnetics Research C*, Vol. 87, 199-212, 2018, 10.2528/PIERC18082902

[11] G. S. Karthikeya, M. P. Abegaonkar and S. K. Koul, "CPW Fed Wideband Corner Bent Antenna for 5G Mobile Terminals", in *IEEE Access*, vol. 7, pp. 10967-10975, 2019, DOI: 10.1109/ACCESS.2019.2891728

[12] L. Cai and K.-F. Tong, "A Millimeter-Wave Aperture-Coupled Simple Low-Profile Magneto-Electric Antenna", *2020 IEEE Asia-Pacific Microwave Conference (APMC), Hong Kong*, 2020, pp. 1078-1080, DOI: 10.1109/APMC47863.2020.9331721

[13] G. Yang, J. Zhang, and Z. Zhou, "Low-Profile Broadband Aperture Coupled Magneto-Electric Dipole Array Antenna for Millimetre-Wave Applications", in *Electronics Letters*, vol.56, no. 6, pp. 271-273, 2020, DOI: 10.1049/el.2019.3514

[14] R. Ketham, A. A. Althuwayb and A. Kumar, "Low-Profile Magneto-Electric Dipole Antenna", in *IETE Journal of Research*, vol. 69, no. 3, pp. 1604–1612, 2021, DOI: 10.1080/03772063.2021.1873200

[15] Z. Mousavirazi, M. M. M. Ali, P. PourMohammadi, P. Fei and T. A. Denidni, "High-Performance CP Magneto-Electric Dipole Antenna Fed by Printed Ridge Gap Waveguide at Millimeter-Wave", in *Sensors*, vol. 24, p. 8183, 2024, DOI: 10.3390/s24248183

[16] S. Shafiq, Y. He, Q. Ali and H. Sun, "A Wideband Dumbbell-Shaped Magnetoelectric Dipole Antenna Array for Ka-Band Applications", in *IEEE Antennas and Wireless Propagation Letters*, vol. 24, no. 12, pp. 4800-4804, Dec. 2025, DOI: 10.1109/LAWP.2025.3612834

[17] C. Q. Zhang and L. Y. Feng, "Design of High-Gain Magneto-Electric Dipole Antenna by Loading a Magneto-Electric Dipole Director", in *IEEE Antennas and Wireless Propagation Letters*, vol. 22, no. 8, pp. 1823-1827, Aug. 2023, DOI: 10.1109/LAWP.2023.3266263

[18] G. Scalise, E. Arnieri, G. Amendola, M. W. Rousstia, S. Pires and L. Boccia, "Dual-Polarized Magneto-Electric Dipole for 5G 28-GHz Phased Array Applications", in *IEEE Open Journal of Antennas and Propagation*, vol. 5, no. 1, pp. 164-179, Feb. 2024, DOI: 10.1109/OJAP.2023.3333232

[19] S. Wu, J. Li, X. Chen, S. Yan and X. Y. Zhang, "A Ka-Band SLM Printed Filtering Divider-Fed Magnetoelectric Dipole Antenna Array Using Embedded Gap Waveguide", in *IEEE Antennas and Wireless Propagation Letters*, vol. 22, no. 4, pp. 774-778, April 2023, DOI: 10.1109/LAWP.2022.3224867

[20] X. Zhong, Q. Li, C. Guo, J. Li, Z. Wang, J. Shi, X. Chen and A. Zhang, "A D-Band Wideband Magnetoelectric Dipole Antenna Array Based on Micro-Metal Additive Manufacturing", in *IEEE Transactions on Antennas and Propagation*, vol. 72, no. 8, pp. 6500-6509, Aug. 2024, DOI: 10.1109/TAP.2024.3423386